Remote Sensing of Environment 204 (2018) 979–996

Contents lists available at ScienceDirect

Remote Sensing of Environment

journal homepage: www.elsevier.com/locate/rse

# Reconstruction of Landsat time series in the presence of irregular and sparse observations: Development and assessment in north-eastern Alberta, Canada

Darren Pouliot[a,*], Rasim Latifovic[b]

[a] Environment and Climate Change Canada, Landscape Science and Technology, Ottawa, Ontario, Canada
[b] Natural Resources Canada, Earth Sciences Sector, Canada Center for Remote Sensing, Ottawa, Ontario, Canada

ARTICLE INFO

*Keywords:*
Landsat
Time series
Sparse sampling
Modeling
Change detection

ABSTRACT

Time series analysis of Landsat is limited by sparse and irregular sampling of clear-sky observations due to acquisition limitations, clouds, shadows, atmosphere, and sensor artifacts. Many remote sensing applications utilizing coarse spatial resolution time series methods are not suitable for Landsat due to observation sparsity. In this research we develop an imputation based approach to constrain the harmonic modeling method of Zhu et al. (2012, 2015) and Zhu and Woodcock (2014b) to reconstruct Landsat time series at a regular temporal interval. The approach was assessed for a boreal forest region in central Canada for different sparsity conditions. The imputed Landsat estimates for a specific pixel were predicted from climate or AVHRR data. These estimates were given a small weight relative to available Landsat observations in fitting the final harmonic model essentially constraining it to a more plausible range. In addition we implemented the model in a piecewise manner to handle non-linear temporal drift related to factors such as climate change, drought, or the allometric nature of vegetation regrowth. Results show that the inclusion of imputed estimates improved model predictions in the presence of observation sparsity. Where there were less than 3 observations within ± 20 days the imputation approach performed better, with a reduction in average reflectance error of 0.001 to 2.5. Error assessment with hold out observations, comparison to MODIS time series, and example predicted images are presented.

## 1. Introduction

Time series analysis has been widely utilized to enhance environmental monitoring and information extraction applications from coarse resolution earth observation (EO) archives. Some common examples are land cover mapping (Borak et al., 2000; Zhan et al., 2000; Pouliot et al., 2013), change detection (Lambin, 1996; Fraser et al., 2005; Lunetta et al., 2006; Hansen et al., 2008; Pouliot et al., 2009a), seasonality (Ramsay, 1998; Zhang et al., 2003; Latifovic and Pouliot, 2007; Zhao and Fernandes, 2009), phenology (White et al., 1997, 2009; Pouliot et al., 2010) and improved cloud and cloud shadow detection (Rossow and Garder, 1993; Cihlar et al., 1999; Lyapustin et al., 2008). With coarse resolution EO data, daily or close to daily measurements of the globe are acquired and thus recognized interpolation methods can be used to generate regularly sampled time series. However, for the Landsat historical record, cloud, haze, shadow, and sensor artifacts combined with the 16 day satellite repeat visit leads to irregular and sparse clear-sky measurements. Generation of regularly sampled time series cannot be easily accomplished with standard interpolation approaches where seasonal properties that change on the order of days to weeks are desired. Thus, time series methods developed for coarse resolution sensors are not suitable for historical Landsat data without some method to provide regularly estimated values.

The degree of irregular and sparse observations varies globally due to several factors other than cloud probability and satellite revisit. Historical Landsat coverage is greatest over the US than elsewhere in the world as shown in Ju and Roy (2008) and Kovalskyy and Roy (2013) due to various trade-offs in acquisition logistics and receiving station capacity particularly with Landsat 5. A mitigating factor is that scene overlap increases towards the poles. At the equator scene overlap is approximately 7% and increases to 80% at ± 80° latitude. Thus, the greater overlap compensates for the satellite repeat visit limitations, but annual seasonal cycles are of shorter duration towards the poles and require greater sampling for adequate characterization. Considering these factors, the more problematic areas for Landsat sampling can generally be identified as regions outside the United States, at low latitudes where scene overlap is minimal, in northerly regions with rapid seasonal development, and where cloud probabilities are largest such as costal zones and mountain regions. Depending on the location, technical implementation of Landsat time series applications may be most

* Corresponding author.
*E-mail address:* Darren.Pouliot@Canada.ca (D. Pouliot).

http://dx.doi.org/10.1016/j.rse.2017.07.036
Received 6 September 2016; Received in revised form 17 July 2017; Accepted 31 July 2017
Available online 06 October 2017
0034-4257/ Crown Copyright © 2017 Published by Elsevier Inc. All rights reserved.

efficiently achieved by an image based approach where overlap is small (i.e. low latitudes) and a pixel based approach where overlap is large (i.e. high latitudes).

Methods to circumvent the sparsity of clear sky observations in Landsat time series are starting to be developed. Pooling observations for several years for phenology assessment has been carried out in Fisher et al. (2006) and Melaas et al. (2013). Methods combining coarse resolution MODIS data with Landsat have also been developed and have shown good performance, but are limited to the temporal extent of the coarse resolution data record (Gao et al., 2006; Hilker et al., 2009; Zhu et al., 2010; Hwang et al., 2011; Emelyanova et al., 2013). In the United States, Zhu et al. (2015) have developed and tested a harmonic modeling approach with considerable success that does not depend on other sensors. The approach has evolved from an initial version intended for change and near-real time change applications (Zhu et al., 2012), has been tested for post-seasonal cloud screening with Landsat (Zhu and Woodcock, 2014a), and for land cover monitoring in Zhu and Woodcock (2014b). In their approach, time series are modeled with harmonic sine and cosine basis, linear trend, and offset terms. The fit is carried out for segments of the time series where land cover change has not been detected. For abrupt changes the time series is modeled separately before and after the change event. In their work the model fit has been determined by least squares, weighted least squares, and regularized least squares approaches to enhance stability and efficiency. Similar to this approach is the B-Fast method developed by Verbesselt et al. (2010, 2012), but a more simplified harmonic based model was required for application to Landsat in tropical forests (DeVries et al., 2015). As stated in Zhu et al. (2015) the minimum sampling requirements are twelve samples to obtain a reliable result. This requirement may be achieved in the US, but in many other regions this could dramatically reduce the applicability of the method, particularly pre-2000, before Landsat 7 was operational. Further, in other regions with shorter seasonal cycles, snow cover, drought and other factors resulting in non-linear drift could result in the model being under-fit and needs to be investigated. An effective strategy to predict regular observations from Landsat for historical analysis is needed to better understand historical land cover, land cover change and seasonality.

### 1.1. Objectives

The objectives of this research were twofold. The first was to improve the accuracy of the harmonic model approach of Zhu et al. (2015) for Landsat modeling in the presence of sparse and irregular clear-sky Landsat observations. The second was to evaluate the accuracy related to sparsity in a northern boreal forest region.

## 2. Data and methods

Due to the multifaceted nature of the research an overview of the main elements of the methodology and the assessments undertaken to evaluate performance are provided in Fig. 1. To address sparse sampling we used an imputation approach to estimate Landsat observations from climate or AVHRR data. These estimated values were used to generate a final harmonic model based prediction using a weighted approach where the imputed values were given a small weight and clear-sky Landsat observations a large weight. The purpose of the imputation was to provide crude estimates to constrain modeling, particularly in regions of sparse observations. It is important to note that a high quality imputed estimate was not strongly required to achieve reasonable results. A second key modification from Zhu et al. (2015) was implementation in a piecewise manner to account for non-linear drift in the time series related to environmental or anthropogenic factors such as climate change, insect damage, allometric nature of vegetation regrowth, or possible pollution effects. To assess performance three evaluations were undertaken: 1) leaving a Landsat observation out for validation, 2) comparison with MODIS time series, and 3) visual evaluation of predicted image outputs. The elements in the figure are discussed in detail throughout the methods section.

### 2.1. Landsat time series

Landsat time series for three adjacent image footprints covering the north-eastern Alberta Oil Sands region of path/row designations 041/020, 042/020, and 043/020 were acquired for the period 1985–2012. Fig. 2 shows the study area and Landsat image footprints. In total there were 1731 Landsat 5 and 7 (L1T, L1G) images downloaded and processed for this analysis. Processing into a standard projection (Lambert Conic Conformal), radiometric calibration, scene identification (cloud, cloud shadow, water, and snow), and quality control was performed using the Moderate Resolution Time Series Data Management and Analysis System developed at the Canada Centre for Remote Sensing (CCRS, Latifovic et al., 2015). This system has been benchmarked against LEDAPS (Landsat Ecosystem Disturbance Adaptive Processing System) processing code and achieves similar performance. The CCRS system was used here as it provided a means to efficiently process, quality control, manipulate and extract time series from Landsat data.

Only the red, near infrared (NIR), and shortwave (SWIR, 1.6 μm) bands were processed as these are known to contain the majority of the data variation in Landsat (Small, 2004) and reduced the overall processing requirements for this research. In addition NDVI was also processed as it is a widely used index and has a sinusoidal seasonality that is well suited to the methodology implemented here. Other indices such as the Normalized Difference Moisture Index have more complex seasonal patterns that may be more difficult to model with harmonic basis (Delbart et al., 2005).

To account for missed and sub-pixel clouds a post-seasonal cloud screening method was applied based on Normalized Difference Vegetation Index (NDVI) time series. The method used a Lowess smoother (Cleveland, 1979) with a window size of 41 days, where values falling below the fit line were replaced with fit values in the final iteration. A window size of 41 was found to provide good generalization that was robust to noise in the time series. Significant deviations were detected as z-scores at the 90% confidence level below the Lowess fit. NDVI of clouds and shadows are known to take on smaller values than vegetated surfaces making it a good index for detection of contaminated values (Holben, 1986; Cihlar et al., 1997).

### 2.2. Coarse resolution earth observation time series

#### 2.2.1. AVHRR data

Time series from the Advanced Very High Resolution Radiometer (AVHRR), High Resolution Picture Transmission (HRPT) 1 km data were used as one auxiliary data source to impute missing Landsat time series values. AVHRR data were processed as described in Latifovic et al. (2005) for calibration, geolocation, cloud screening, and compositing. Sensors used included NOAA-9, 11, 16, 17 and 19. Additional cross-sensor calibration for AVHRR sensors 2 and 3 was applied as described in Latifovic and Pouliot (2013). Composites were produced at 10 day intervals from 1985 to 2012. The red, NIR, and surface temperature measurements were used in modeling.

#### 2.2.2. MODIS data

Moderate Resolution Imaging Spectroradiometer (MODIS) time series were used as a benchmark for comparison of the predicted Landsat results for the period 2000–2012. TERRA Level 1B geolocated top of atmosphere radiance (MOD02) data were processed following the procedures described in Trichtchenko et al. (2006) for downscaling of 500 m resolution bands to 250 m, Khlopenkov and Trichtchenko (2008) for resampling of the latitude and longitude fields to the Canada Lambert Conformal Conic projection, and Luo et al. (2008) for compositing to 10 day intervals. Only the SWIR band 6 of MODIS was

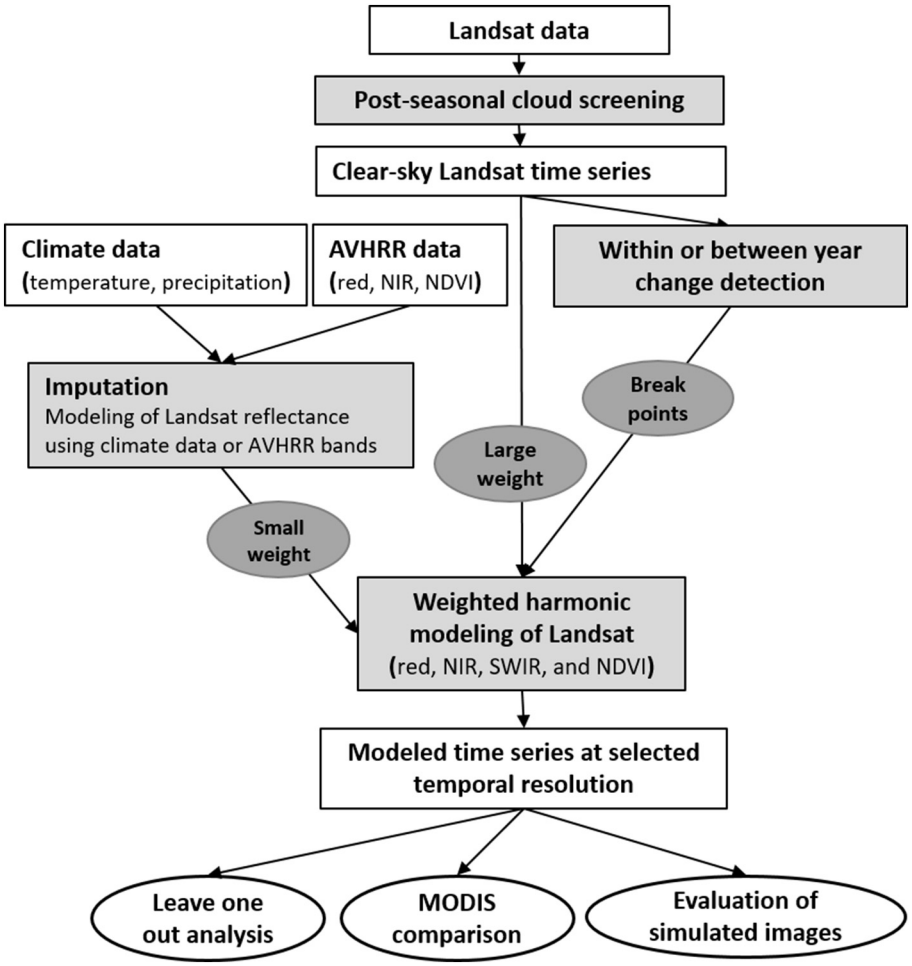


**Fig. 1.** Overview of the methods and evaluations undertaken. White boxes in the figure represent data inputs/outputs, grey boxes represent processing methods, and white circles are the different evaluations undertaken.

downscaled. The red and NIR bands were used at their native resolutions of 250 m.

### 2.3. Climate data

Daily climate station data for Fort McMurray were acquired for the period 1985–2012 and used for imputing missing Landsat observations. To test the concept presented here a single station was considered sufficient for the extent of the study area. However, for large regional implementation additional stations would likely enhance accuracy. The selected station was the most complete in terms of record continuity and had the fewest missing observations within the study area. Fig. 2 shows the location of the monitoring station within the study area depicted by the star. Missing temperature data in the time series were linearly interpolated. Missing precipitation could not be easily interpolated and thus were left as missing. There were only a few missing observations in the time series records for temperature (2%) and precipitation (3%).

### 2.4. Piecewise harmonic time series modeling

Following from Zhu et al. (2012, 2015) and Zhu and Woodcock (2014b) we used the following model to predict Landsat reflectance for a specific band:

$$\rho_i = c_{0,i} + c_{1,i}\cos\left(\frac{2\pi}{T}x\right) + c_{2,i}\sin\left(\frac{2\pi}{T}x\right) + c_{3,i}x + \varepsilon_i \quad (1)$$

where,

$x$ Julian day starting in 1980

$i$ Landsat band

$T$ number of days in a year (365.25) to account or leap years

$c_{0,i}$ offset coefficient

$c_{1,i}, c_{2,i}$ coefficients to account for annual seasonality and phase

$c_{3,i}$ coefficient for linear trend

$\varepsilon_i$ error

In Zhu et al. (2015) the above model was fit to segments of the time series where abrupt land cover change was not detected. Depending on the available observations the number of harmonic terms was increased to enhance the model fit. If there were 6–18 clear-sky observations model (1) was applied, between 18 and 24 observations additional terms, $c_{4,i}\cos\left(\frac{4\pi}{T}x\right)$ and $c_{5,i}\sin\left(\frac{4\pi}{T}x\right)$, were added to account for within year variability and if more than 24 observations were available two more terms were added to account for greater within year fluctuations, $c_{6,i}\sin\left(\frac{6\pi}{T}x\right)$ and $c_{7,i}\cos\left(\frac{6\pi}{T}x\right)$.

Model (1) can be fit using a variety of methods to trade-off between accuracy, noise sensitivity, overfitting, and processing speed. In Zhu et al. (2012) and Zhu and Woodcock (2014b) least squares and robust least squares regression methods were used. For their recent work they have used the LASSO (least absolute shrinkage and selection operator) regularization approach to avoid overfitting (Zhu et al., 2015).

In our implementation, to account for potential non-linear drift in the time series occurring over multiple years and improve the overall fit, we apply model (1) in a piecewise manner. Models were developed separately to predict the Landsat measurements in each year using three years of data which included the adjacent years. The model was fit using robust least squares regression with the Tukey biweight (Press et al., 1992). For each three-year segment of the time series, the data for central year was given the largest weight and bounding year's smaller

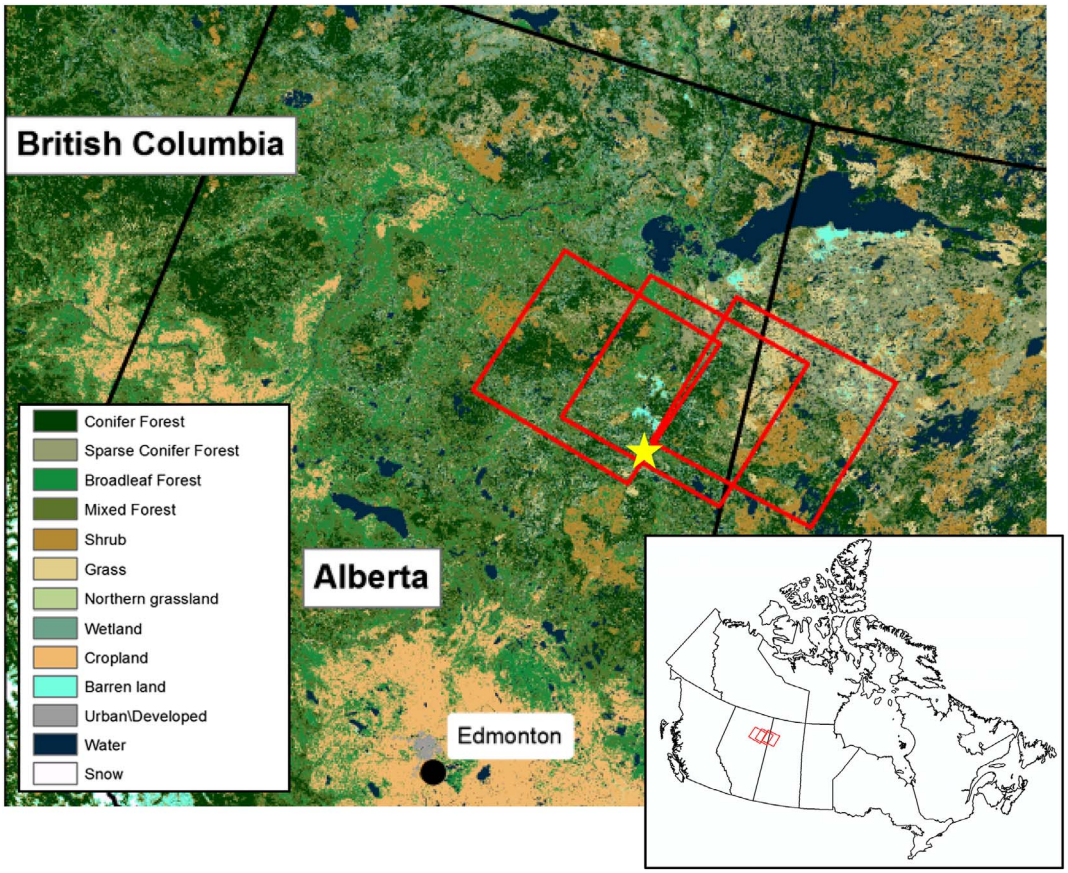


**Fig. 2.** Study area. Land cover data shown is the 30 m Land Cover of Canada 2010. The star in the figure denotes the location of the climate station data used. The Landsat footprint path-rows are 42–19, 42–20, and 42–21. The center of the study area is located at 56°03′ North and 110°46′ West.

weights. Depending on the degree of noise and observation density, weights can be adjusted for the data in adjacent years. We found weighting the data for the central year with 1 and adjacent years by 0.3 gave a reasonable trade-off between fit, robustness to noise, and sparse observations. In our initial work, we tested standard L1 and L2 regularization techniques, but found that in the presence of sparsity the seasonality coefficients in model (1) were removed or heavily reduced resulting in an overly simplified fit.

### 2.5. Change detection

Model (1) does not explicitly account for abrupt changes. To address this in Zhu et al. (2012, 2015) and Zhu and Woodcock (2014b) change was detected as a deviation from an initial model of the time series. This requires a stable segment of the time series where change has not been detected for model development. Identification of a suitable segment of the time series for this purpose is not trivial and can have a substantial effect on the results if selected incorrectly. Once developed, abrupt change can be detected by comparing model predictions with observations to determine if there is a sufficient deviation.

For our piecewise implementation we developed two approaches for detecting change based on the Zhu et al. (2015) approach. The first was within year change, where a land cover change during the year was detectable. The ability to detect this type of change was dependent on the availability of sufficient clear-sky Landsat observations. The second approach was change only detectable between years. This occurred because there were too few observations for reliable within year detection or the change took place early or late in the growing season and thus the change signal was small due to the leaf-off conditions.

#### 2.5.1. Within year change

To account for within year change model (1) was fit without the trend term to the time series for a single year. Residuals between the Landsat observations and model predictions were computed and converted to z-scores ((residual-mean)/standard deviation). A median filter was applied with a moving window size of 21 days. The median filter was applied to preserve persistent edges in the time series and reduce noise. It is not essential to apply, but can help to reduce commission error. If the filtered results exceeded the change threshold it was accepted as change and the date recorded as the change break point. This within year change method accounted for rapid changes in the time series during the growing season. Fig. 3 shows an example of the model adaptation to within year change caused by a fire in 2005.

We empirically determined that the z-score change threshold should be between 1.6 and 2 depending on the commission\omission error tolerance. We settled on a value of 1.7 as a suitable compromise that was predisposed towards omission error. Omission error was preferred to avoid overfitting in the presence of noisy Landsat observations. All bands were tested to determine if change occurred and accepted if any band passed the threshold criteria.

If within year change was detected, the time series modeling was carried out separately before and after the date of the detected change (i.e. break point). However, this was only applied if there were at least 10 observations in the year and more than 5 observations (including the adjacent years) on either side of the detected break point.

#### 2.5.2. Between year change

To detect changes that were evident between years we modeled the three year time series segment using model (1) without the trend term, but weighted the center year observations the largest with 0.9 and adjacent years with 0.25. This weighting ensured a good fit for the data

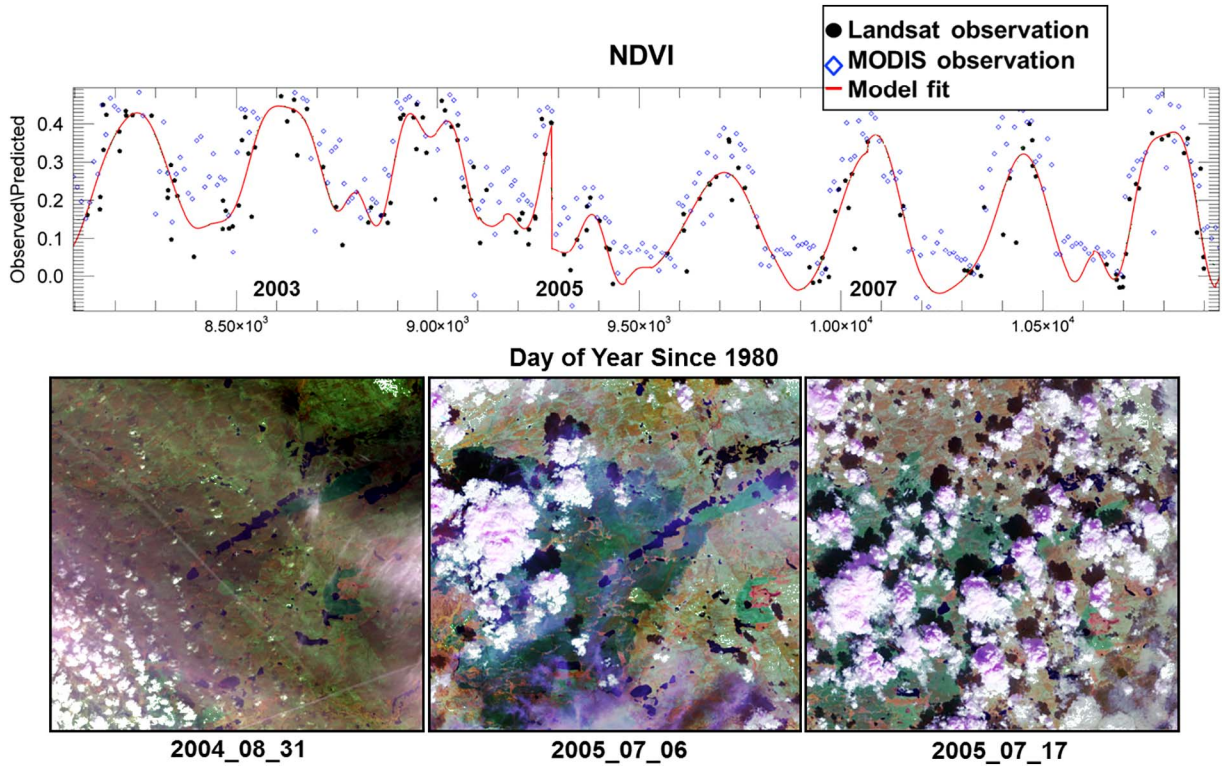


**Fig. 3.** Example of within year change detection associated with a fire in 2005. Images are Landsat showing the fire before and after change. Images are displayed as red = NIR, green = SWIR, and blue = Red. The fire is identifiable as the dark green object in the 2005 image examples.

in the year being predicted. The median of the z-score residuals between the model predictions and observations were computed for each year. If the median z-score for a year was greater than the specified threshold it was removed and the modeling of the data for that year proceeded with only two years. Taking the yearly median to determine change required the z-score threshold to be lowered to 1.3 as this approach was less sensitive to detecting change. A balance of omission and commission error was preferred, but the model can adjust to missed changes that are of small-magnitude, relative annual increase or decrease of 30% reflectance or less.

If the Landsat observations for the two adjacent years deviate from the central year and are detected as change then a 2nd order polynomial term ($c_{n,i}x^2$) was added to model (1) if there were at least 10 observations for the year being modeled. This accounted for potential annual drought or other stress events that could cause the central year's data to deviate from its neighbors. Fig. 4 shows an example result of the drought type condition in Fig. 4A and change detection of a forest harvest in Fig. 4B.

### 2.6. Imputation and constrained time series modeling

To constrain the harmonic model, climate and AVHRR data were used as sources for regression based imputation of Landsat reflectances. The following describes the two approaches tested. Climate station measurements of maximum daily temperature and precipitation were used to model Landsat reflectance as:

$$\rho_i = c_{0,i} + c_{1,i}T + c_{2,i}T5 + c_{3,i}P + c_{4,i}x + \varepsilon_i \quad (2)$$

where,

$T$ mean temperature for the preceding 30 days.

$T5$ mean temperature above 5 °C for the preceding 30 days.

$P$ total precipitation for the preceding 30 days.

Substantial experimentation was undertaken to evaluate different temperature and precipitation features that could be extracted from the daily data and used for modeling. The 30 day criterion was selected largely because it was the minimum that provided a sufficient reduction in the daily fluctuation so that model results were stable. The threshold of five degrees was selected based on the concept of growing degree days where this value is considered suitable for general plant growth (Edey, 1977).

Model (2) was fit using robust least squares regression with the Tukey biweight. However, to find the simplest model, the full model was compared with subset models of two variables. The mean squared error was calculated for all models and the percent difference relative to the full model was determined. The model with the smallest difference was selected if it was within a threshold of 10% of the full model. The selected model was used to predict new observations to densify the time series for fitting the final harmonic model to available clear-sky Landsat observations (model (1)). These predicted values were given a smaller weight than the Landsat observations. The selection of the weights controls how closely the final result mimics the imputed climate based estimates. In our experimentation a value of 0.25 worked well allowing the final model to deviate from the climate based estimates as needed. The degree of densification of the time series with imputed estimates also needs to be considered. High densification or large weights will reduce the sensitivity to the Landsat observations. We densified our time series by estimating values every 16 days to provide two values per month, which worked well with the weight set at 0.25. For winter, the weights were given a smaller value of 0.15 because there are generally very few clear-sky winter observations in the time series and we have reduced confidence for their retrieval. Fig. 5 provides an overview of the constrained harmonic method applied here for an open conifer forest in 1989. The climate features are clearly correlated with Landsat NDVI in this case.

AVHRR data was used in a similar manner as climate, but was modeled as:

$$\rho_i = c_{0,i} + c_{1,i}R + c_{2,i}N + c_{3,i}St + c_{4,i}x + \varepsilon_i \quad (3)$$

where,

$R$ red reflectance AVHRR channel 1

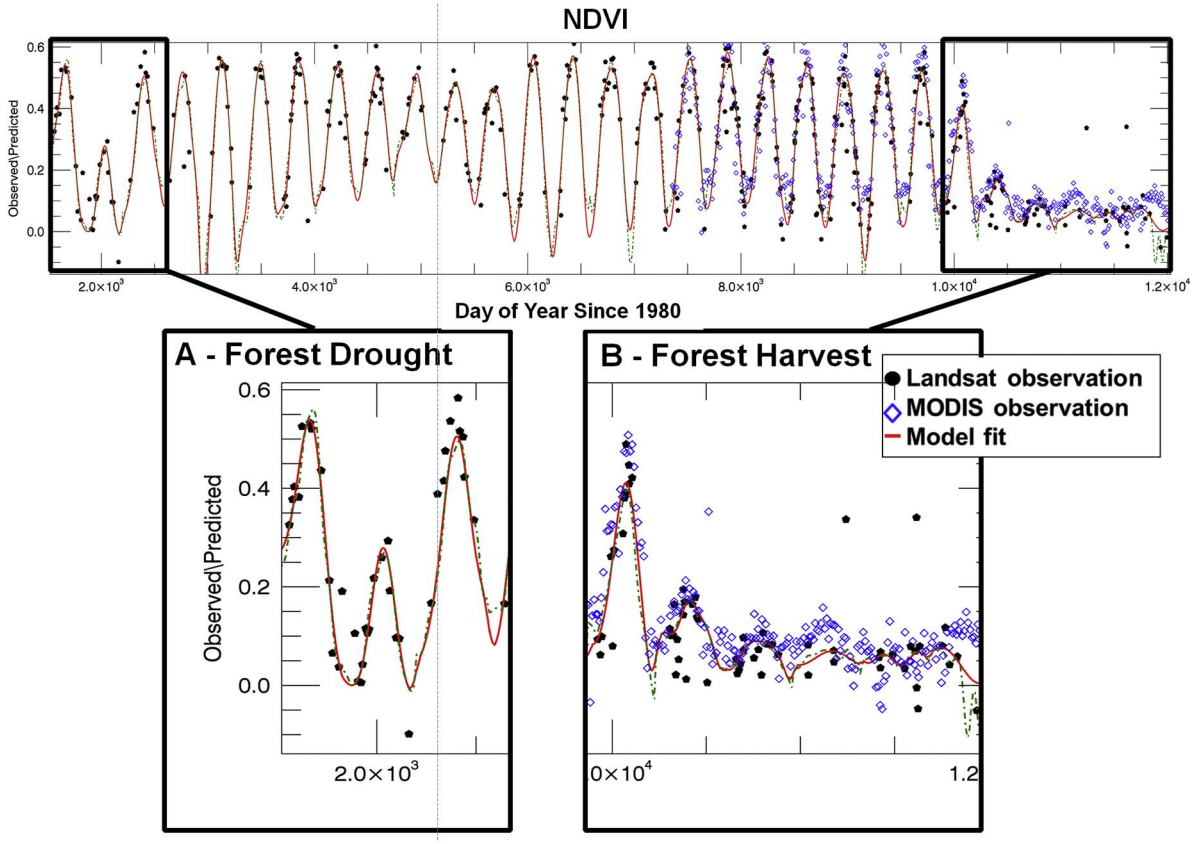


**Fig. 4.** Example results for between year change. In A) the model fit to an anomalous year or drought type condition. In B) forest harvest detectable between years.

*N* NIR reflectance AVHRR channel 2
*St* surface temperature

AVHRR time series were filtered to remove residual cloud and shadow in the 10 day composites. Lowess filtering of the time series was applied with a 41 day window size. Two iterations were performed where for red and NIR bands values greater than 25% of the Lowess fit were replaced with the filtered values. As clouds and haze are often the dominant source of unwanted variation, selection for smaller values tends to provide a good result. It is the basic principle behind the time series processing used in Latifovic and Pouliot (2007), Pouliot et al. (2009a), and Zhao and Fernandes (2009). Selection for larger values was applied for surface temperature. AVHRR tends to contain substantial noise related to the field of view, sun-sensor geometry, and residual clouds and cloud shadows (Pouliot et al., 2009b). Thus, to achieve good generalization of the time series a final Lowess filter was applied with a 31 day window size. Various windows sizes were tested ranging from 31 to 71 days and results varied little. Lowess applies a locally weighted linear regression and thus points closer to the point of estimation have much more weight than those further away (Cleveland, 1979).

The constrained modeling case described above artificially increases the ratio of Landsat observations to model parameters possibly allowing for more complex models to be used and a better overall fit to the data. Thus the clear-sky observation thresholds used by Zhu et al. (2015) to add additional harmonic terms to model (1) were modified as: less than 9 observations model (1) was used, between 9 and 18 observations the $\left(\frac{4\pi}{T}x\right)$ terms were added, and greater than 18 observations the $\left(\frac{6\pi}{T}x\right)$ terms were added.

### 2.7. Assessment

#### 2.7.1. Leave one out analysis

For the leave one out quantitative comparisons 108 time series were randomly sampled by land cover and change occurrence. Land cover and change data used in the sampling were from Pouliot and Latifovic (2016) with reported accuracies of 70% and 89% respectively. Nine land cover types were used. These and their percent areas in 2012 were needleleaf forest (17%), sparse-needleleaf forest (15%), mixed forest (5%), broadleaf forest (14%), shrub (16%), herbaceous (14%), bare (10%), wetland (4%), and water (5%). For each land cover type six time series were sampled where change was not detected and six where change was detected. Between 1985 and 2012 approximately 35% of the area was found to have changed (Pouliot and Latifovic, 2016).

The leave one out statistical assessment was applied to the Landsat time series where, for each year, one observation was removed at random. The time series segment was modeled and the prediction and actual measurement left out were compared. For each year, ten iterations were carried out. Thus in total there were (10 iterations × 29 years × 108 time series) = 31,320 paired comparisons for analysis. The error analysis included histograms of differences by method and band\feature; mean absolute error (MAE) by method, band\feature and land cover; MAE relative to observation density, and class weighted MAE (WMAE) using the percentages specified above. Observation density was measured as the number of clear-sky Landsat observations within ± 20 days of a given day in the time series. Different day ranges were tested from 10 to 30, and results were similar among them. The main advantage of using a larger day range was that it increased the range of output observation densities.

To evaluate the modeling performance in the presence of change we computed the leave one out errors for time series containing abrupt changes. We randomly sampled 60 time series where abrupt change occurred resulting from forest harvesting, fire, or industrial development. We compared error statistics within plus or minus one year of the detected changes. This range was used to account for the temporal detection error identified in Pouliot and Latifovic (2016). Detection of change was not the objective in this work, but rather model performance in the presence of change.

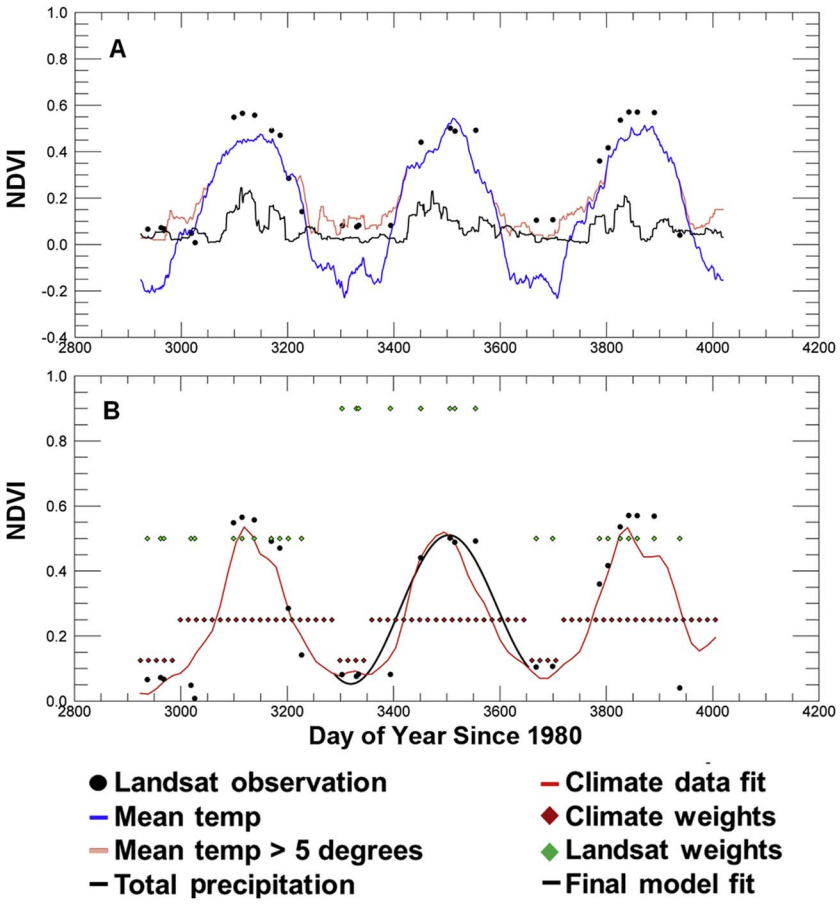


**Fig. 5.** Overview of the constrained harmonic time series modeling. In A) Landsat NDVI and extracted climate features are shown scaled from − 1 to 1. Symbols are given on the left. In B) the result of modeling using model (2) is shown in red along with the weights selected for the final fit. The black line is the final harmonic fit using model (1) and the imputed climate estimates and selected weights. Symbols are specified on the right.

#### 2.7.2. MODIS comparison

To facilitate the MODIS comparison at 250 m spatial resolution, 54 time series were randomly sampled by land cover type for areas that were homogenous within a 9 × 9 sample window at 30 m spatial resolution. Comparison to MODIS data provided an additional means to assess results, particularly to account for segments of the time series with few Landsat observations. MODIS time series were filtered to remove residual cloud and shadow in the 10 day composites following the method applied to AVHRR. Comparison between the predicted Landsat and MODIS time series was assessed for absolute error and correlation for the three bands and NDVI.

#### 2.7.3. Visual assessment

Various comparisons of the predicted images were made as it readily allows for identification of the spatial distribution or error related to cover type or specific reflectance properties. For visual comparison we show examples of the different methods over multiple years, throughout a season, and relative to Landsat images acquired close to the modeled image date.

## 3. Results

### 3.1. Leave one out analysis

Histograms and WMAE of the leave one out analysis for the selected features are shown in Fig. 6 for the different methods. The tighter the spread around zero error indicates the best results or the lower WMAE. The SWIR band had the smallest absolute error. This was principally due to the smaller seasonal range (summer to winter reflectance difference) of the time series that the model was required to capture. In contrast NDVI had the largest error which was related to the greater seasonal range of NDVI data (− 1 to 1). Comparison of the different methods revealed that for all features the constrained methods (climate and AVHRR) had the smaller errors. Climate had slightly smaller error than AVHRR for most cases. The largest improvement was found for the red and NIR bands.

Example NDVI results for the different methods between 1990 and 1999 for a broadleaf forest pixel are shown in Fig. 7. The period 1990–1999 was selected as it is more likely to be sparsely sampled as only Landsat 5 was operational at the time. As can be seen in the figure the unconstrained results tend to fall short or exceed the Landsat observations more frequently and tend to be more sensitive to noise.

Example NDVI time series modeling results for the period 1997–2003 are shown in Fig. 8 for selected land covers and features. Only the climate constrained results are shown as it was found to have slightly reduced error compared to the AVHRR constrained. These examples show that the final harmonic model fit the Landsat observations well in most cases and did not strongly follow the climate based estimates when in error. The largest errors tend to occur in winter as there were very few clear-sky Landsat observations (Goward et al., 2006).

#### 3.1.1. Influence of sparse sampling

The leave one out error results relative to observation density are shown in Fig. 9. For all features error decreases with more observations as expected. The biggest effect was on the red and NIR bands. NDVI was similar but with slightly less magnitude. The effect of the constrained modeling showed that for both AVHRR and climate, the error was reduced for observation densities ranging from 0 to 3. Climate based imputation had the smallest error when the observation density was zero. Approximately 90% of the data was contained in the 0–3 observation density range and 55% in the 0–1 range. The increase in error standard deviation for the red and NIR bands for observation densities greater than 5 is a consequence of the small number of samples.

To examine the influence of sparsity on specific land covers and

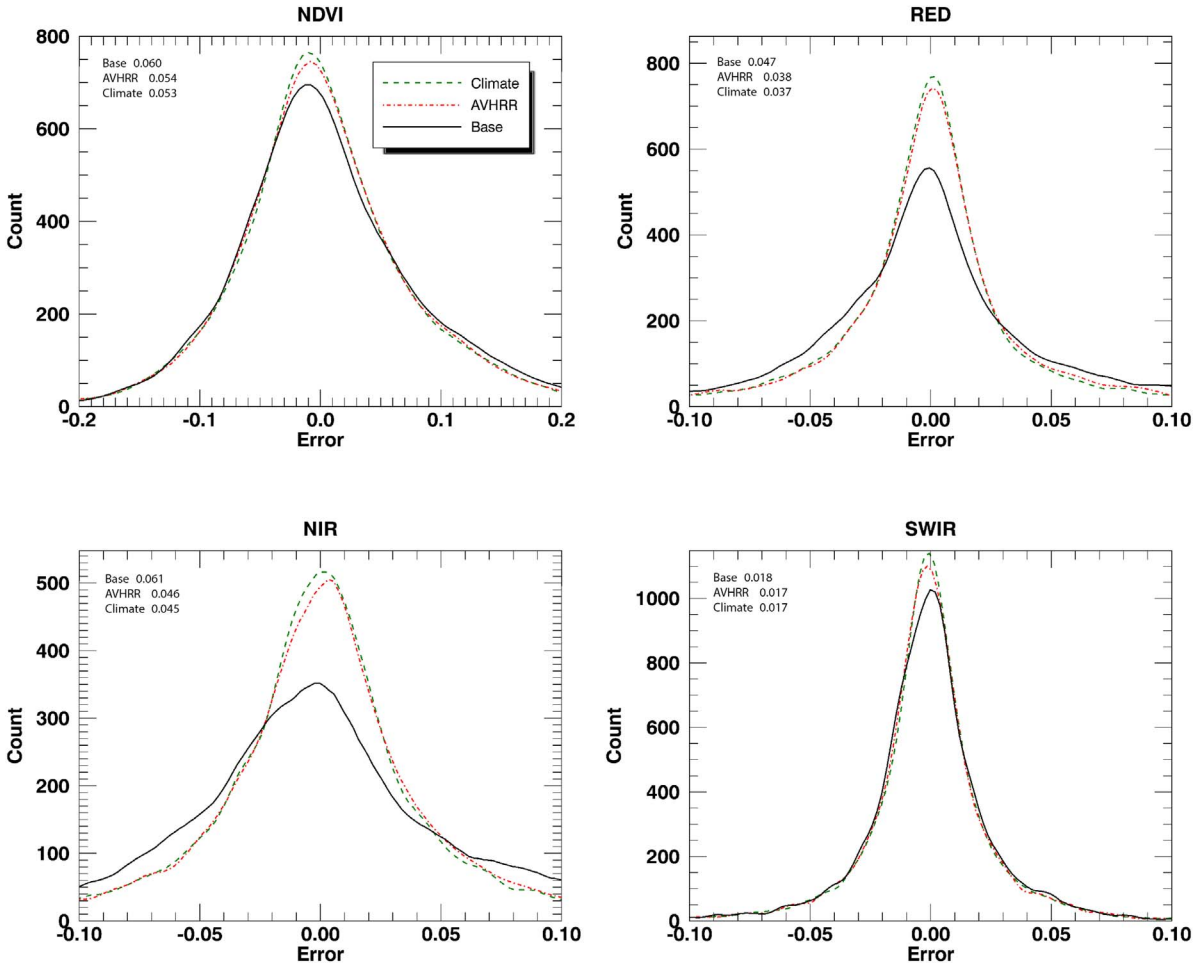


**Fig. 6.** Histograms of errors for the leave one out analysis. The WMAE is given in the top left of each plot.

features, the mean absolute error was calculated for observation densities greater than 2 (high density) where the influence of sparsity was found to be small and less than or equal to 2 (low density) where a stronger effect was observed. Fig. 10A–B shows the results. For both density categories the same general results were found, but with reduced error magnitude for the high density case.

The error magnitudes observed were largely related to the reflectance standard deviation by cover type and feature (Fig. 10C). Basically the more variable a time series is, the more difficult it was to model. Variability was related to noise and seasonality of the time series. The unconstrained method had the largest error across all land cover types and features. It also showed the biggest change between the high and low observation densities. The climate constrained results had reduced error relative to the AVHRR constrained for the low density case. For high density, the difference between the two methods was negligible. Regarding land cover, water generally produced the largest error. Water has the greatest reflectance contrast between summer and winter (water vs. ice/snow) and thus was more difficult to capture in the presence of sparse observations. For the reflectance bands, forested classes tended to have reduced error relative to non-forested, largely because of smaller winter reflectance associated with trees and tree shadows on the snow cover.

Investigation of the difference between the AVHRR and climate constrained results suggests it was related to cloud probability. In Canada fall and winter tend to have greater cloud probability than spring and summer (King et al., 2013). Thus, there are fewer clear-sky Landsat and AVHRR observations in fall and winter leading to larger potential model error for the AVHRR constrained results as shown in Fig. 11. Only the red band is shown as the results for the other bands were similar, except for the SWIR, where there was little difference between methods (Fig. 10). These results provide an explanation for the climate and AVHRR results shown in Fig. 9, where the difference for low observation densities appears to be related to a greater probability of clouds and cloud shadows in the fall and winter.

### 3.1.2. Model performance in the presence of abrupt change

For the abrupt change sampled time series the leave one out error analysis showed that there was a slightly larger prediction error for years with change than years without based on the 5th and 95th percentile errors (Fig. 12). The mean and 25th and 75th percentiles showed negligible differences. The likelihood of having larger error for years with change is logical given that change presents a more complex signal and the use of data for adjacent years to control the fit is reduced. In the presence of sparse observations this is further intensified. Results here suggest only a small difference in error relative to sparsity or land cover/feature effects (Fig. 10).

## 3.2. MODIS comparison

Comparison with MODIS provided another means to assess the model performance independently. Results of the MODIS comparison show that it was similar to the leave one out analysis (Fig. 13A). The constrained results have smaller error in almost all cases. However, the differences between the AVHRR and climate results are not as pronounced as the leave one out analysis suggests.

The correlation analysis revealed that NDVI was the most correlated

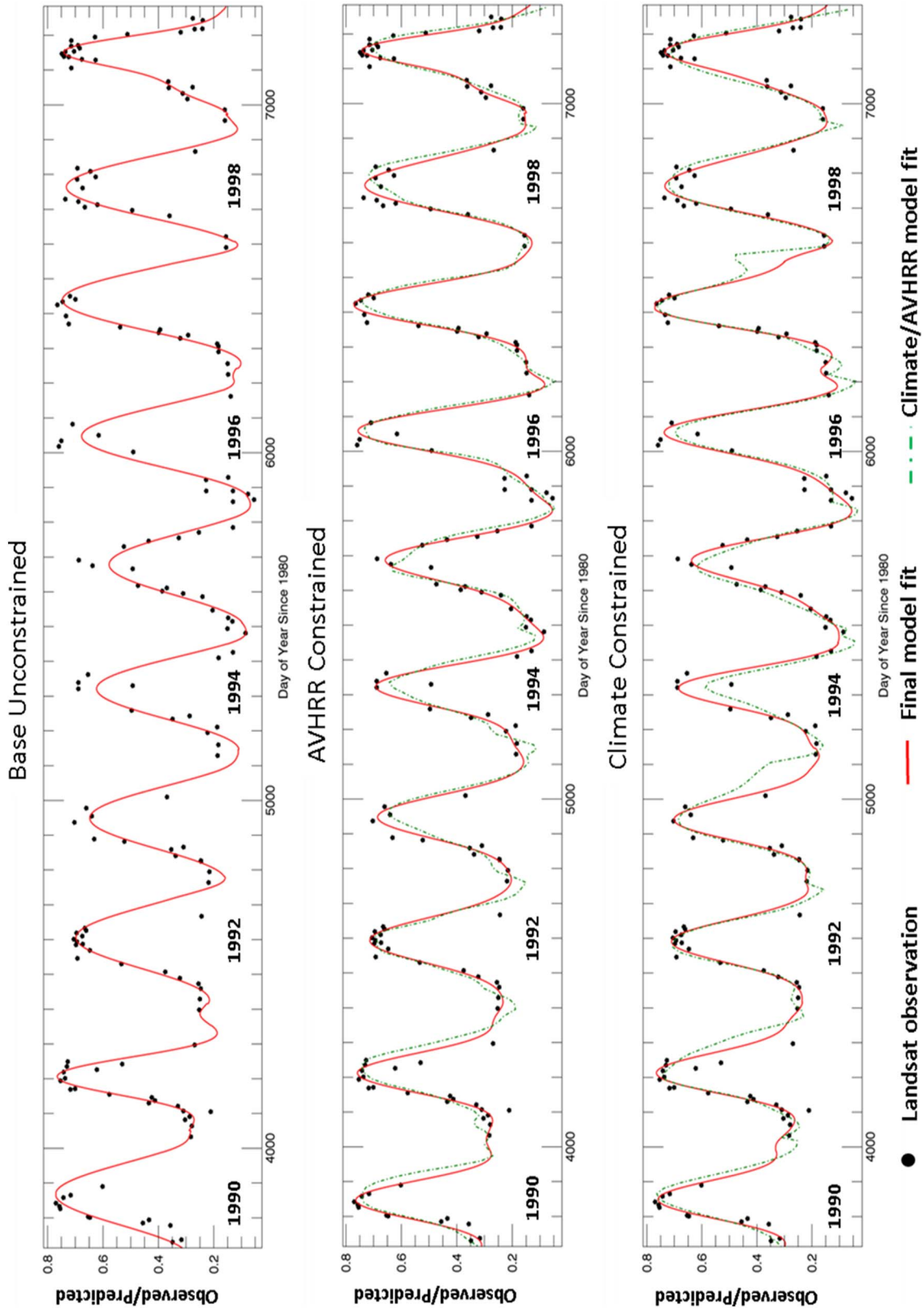


**Fig. 7.** Example NDVI time series for a broadleaf forest pixel from 1990 to 1999. Black dots are Landsat observations, red line is the harmonic model fit, and the green line is the AVHRR or climate based fit used to densify the time series.

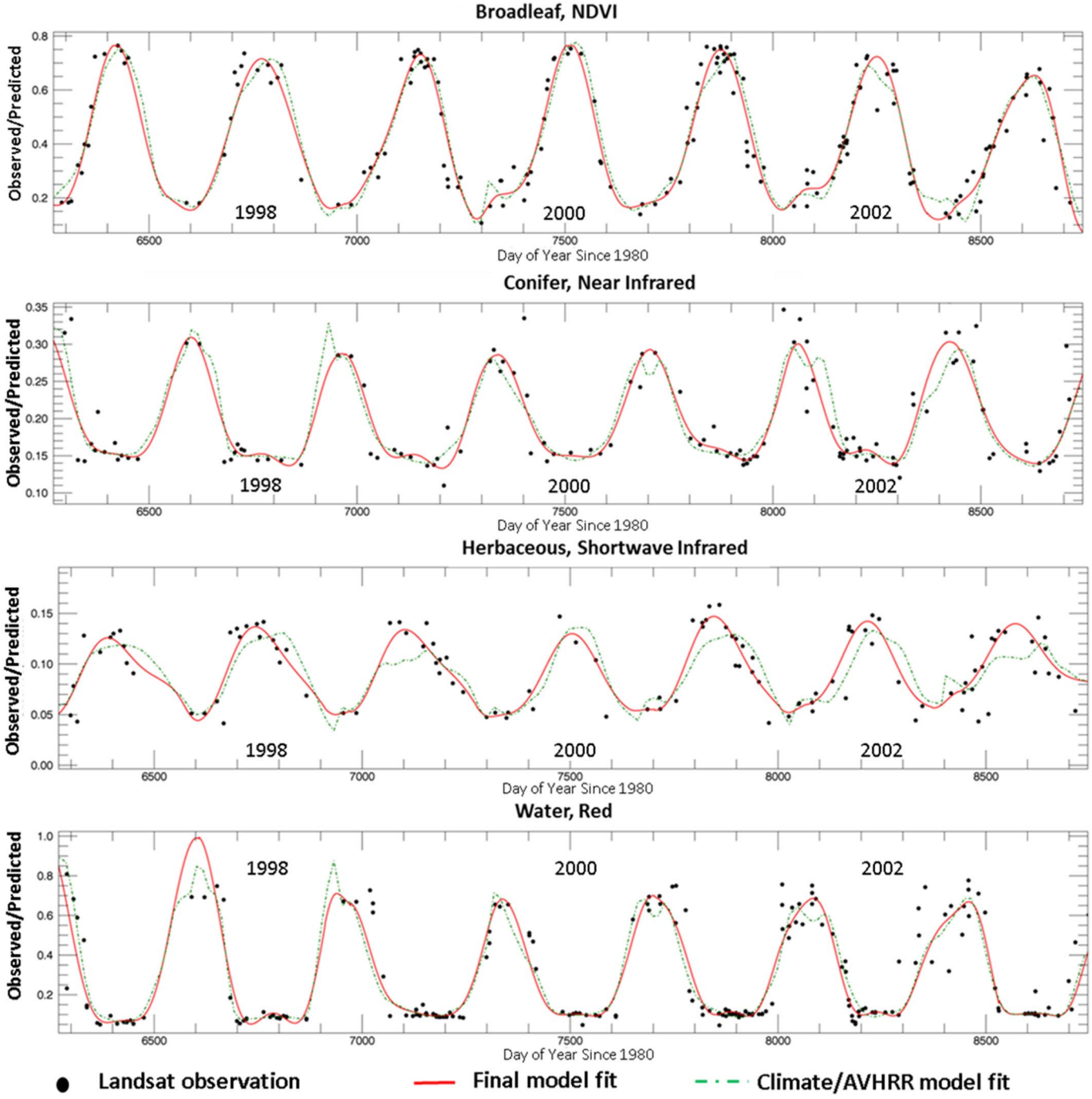


**Fig. 8.** Example time series and climate constrained model results for different data features and land cover types. Note snow/ice are present for each example in winter.

feature for vegetated cover types whereas bands tended to have smaller correlation (Fig. 13B). NDVI for vegetation covers has strong seasonality which is well characterized by the sinusoidal basis function used in the models. Larger error for water and small correlation for water with NDVI was expected as NDVI is not a suitable feature for water characterization. For some cover types and feature combinations small correlations were observed, largely because the time series data had more complex seasonal structure. This occurred mostly for the NIR and SWIR bands and was related to the similar reflectance properties for snow in winter and vegetation canopies in summer. Although a small correlation was observed, the error was small because the seasonal range of reflectances were reduced.

### 3.3. Example predicted images

Several example images were generated to show comparison between methods, model predictions relative to true Landsat measurements, and the predicted seasonality. Fig. 14 shows a comparison between the constrained and unconstrained predicted images for different years. For this example the fall senescence period was selected as there is greater vegetation change and larger cloud probability. Thus, error related to sparse sampling is more likely to arise. The effect of sparse observations is clear in this figure with the 1985 and 1990 examples showing much greater image noise than the more recent examples. For the 1985 and 1990 images 0 or 1 observation was within ± 20 days of

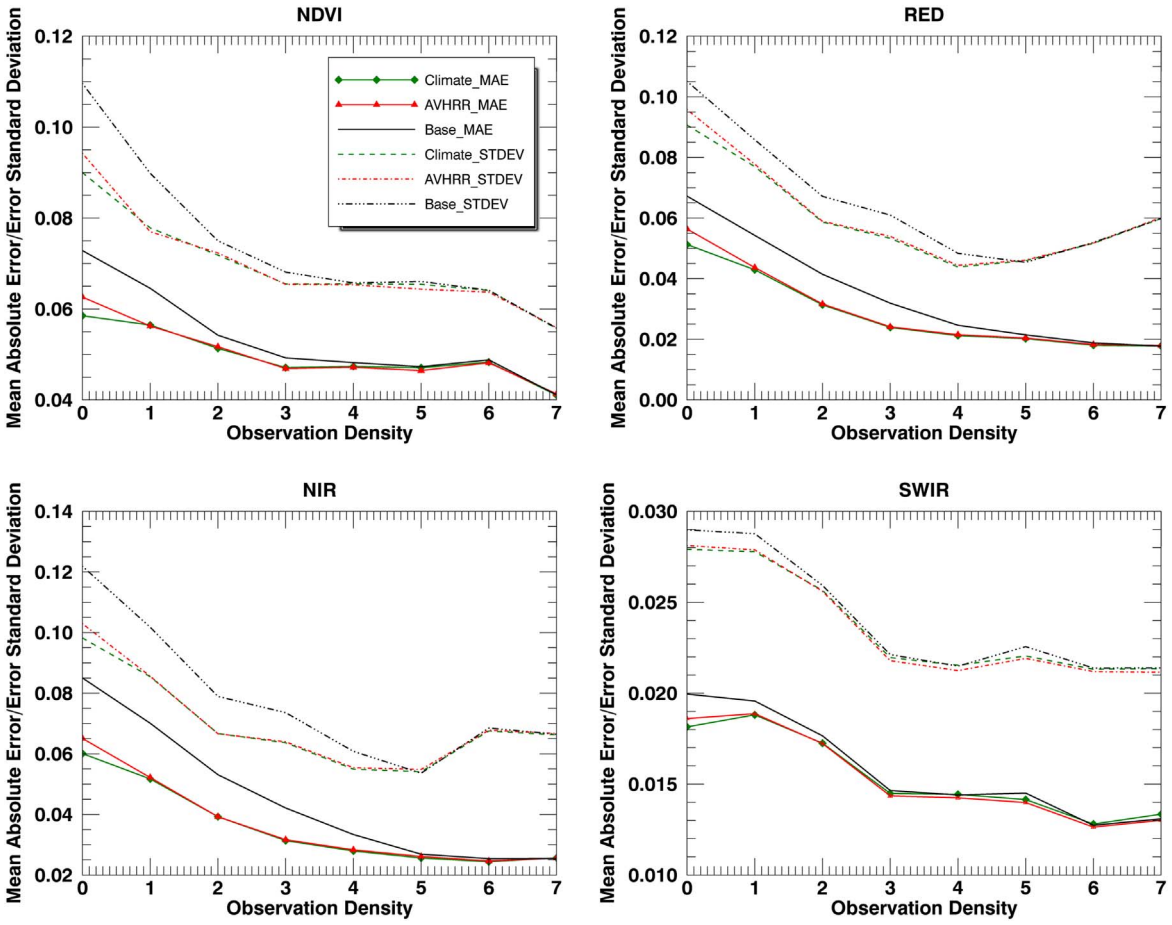


**Fig. 9.** Relation between observation density and mean absolute error/error standard deviation and data feature.

the September 20th date selected. For the 1995 to 2010 examples spatial noise was less apparent and observations density was larger in the range of two or more. Consistent with previous results the climate constrained results appear to have reduced noise the most for the 1985 and 1990 results.

Comparison with the nearest three Landsat scenes revealed good agreement in the clear-sky regions (Fig. 15). Here we show examples for each season (spring, summer, fall, winter). As expected summer had the smallest error because of the availability of clear-sky Landsat measurements and it represents a period where vegetation is generally more stable compared to the spring or fall. The predicted spring image example shows a greater amount of vegetation than the closest clear-sky neighboring Landsat scene would suggest. Offset errors in the rates of green-up or senescence are likely due to limited clear-sky samples characterizing the critical development phases. The results for winter are reasonable for this example, showing a good blend of the two neighboring scenes. As noted previously winter was difficult to model due to cloud cover and limited sampling (Goward et al., 2006).

In Fig. 16 we compare a larger example region for seasonal development and change between 1986 and 2010. This shows different changes and regrowth that occurs for the three seasons of spring, summer, fall. On the far left of the image a large forest fire can be seen that regenerates to broadleaf and mixed forest from 1985 to 2010. Patches of understory conifers can be seen in the fall imagery for 2010 that are harder to identify in the summer image, particularly in the forest cutovers.

## 4. Discussion and conclusions

Reconstruction of a high quality Landsat time series for the period 1984-present is an important objective to develop information for understanding the role of historical land surface change on environmental processes such as air quality, weather, climate, biochemical cycling, hydrological cycling, and wildlife population dynamics to name a few. In this research we sought to augment the existing harmonic approach of Zhu et al. (2015) by imputing additional observations to constrain final reflectance predictions. The developed approach has shown to enhance the results in the presence of substantial sparsity. As a general approximation we find that the imputation approach improved results where there were fewer than three observations within ± 20 days of the date being modeled. Where there were sufficient observations, three or more, the imputation approach did not provide a notable advantage. Using climate data for imputation was found to have slightly reduced error compared to using AVHRR. AVHRR and Landsat are similarly affected by clouds leading to low quality or sparse observations during periods of high cloud probability. Based on statistics for the study area this occurs mostly for the fall and winter.

The results obtained here have similar error magnitudes to those reported in Zhu et al. (2015) where for Landsat bands errors generally ranged from − 0.1 to 0.1. It is important to note that the results presented are strongly influenced by snow/ice in winter which greatly enhances the seasonal range of reflectance to be predicted. Despite this there is good general agreement between these results and those reported in Zhu et al. (2015). These errors may appear large for some applications, but is important to note that it is not consistent in magnitude or direction and balancing of error between time series points

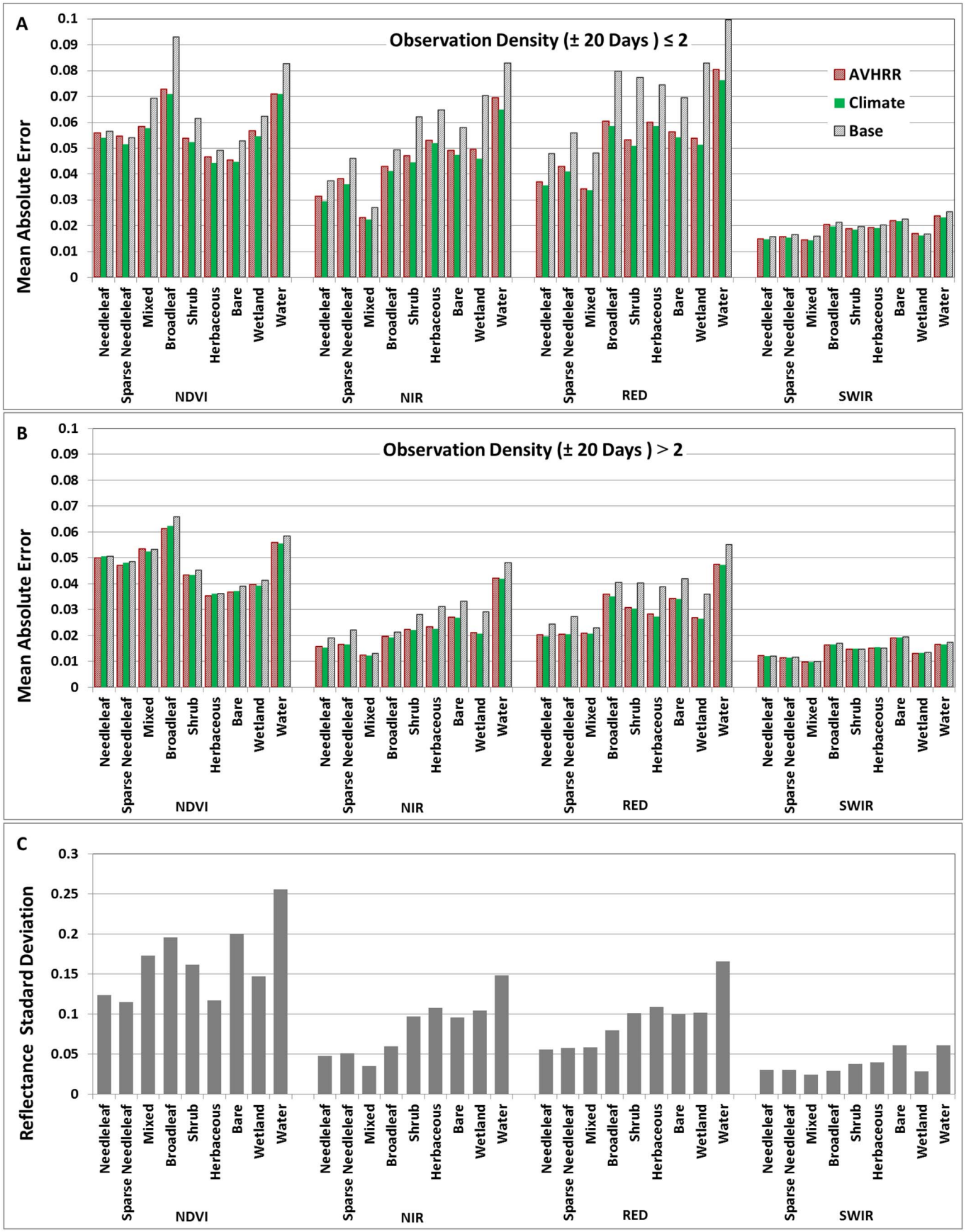


**Fig. 10.** Absolute error from the leave one out analysis by cover type for observation density less or equal to 2 within ± 20 days (A) and greater than 2 (B). In (C) the standard deviation of the reflectance for each land cover feature combination is shown.

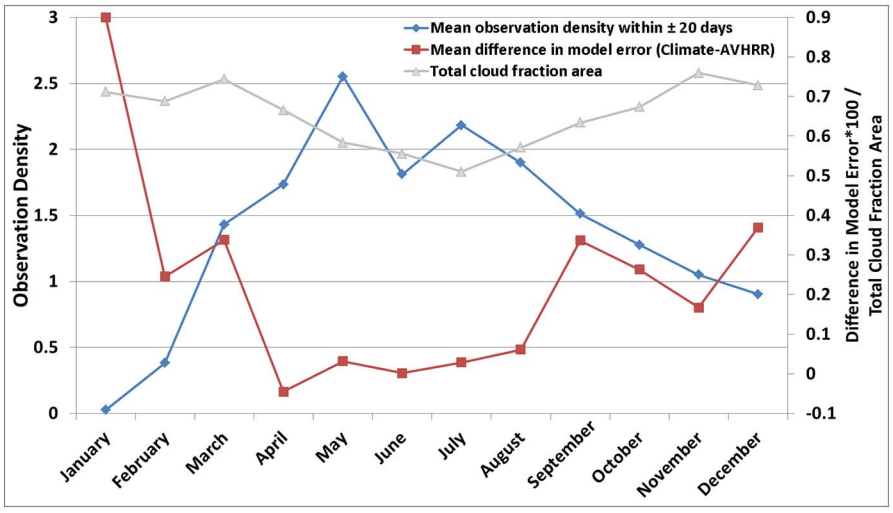


**Fig. 11.** Mean absolute difference in model error for the red band by month and relation to cloud and observation density. Cloud fraction data was taken from the Giovanni web-service averaged from 2006 to 2008 for the study area.

may reduce the impact for some applications. Visual examination of the predicted images produced show that the general spectral characteristics of land covers are maintained and suggest considerable potential for land cover and land cover change applications as examined in Zhu and Woodcock (2014b). An important point here is that the error assessment is not without limitations. Comparison of predicted results with independent Landsat observations could inflate error related to Landsat processing such as sensor calibration, cross calibration, geolocation, cloud and shadow detection, and haze or other atmosphere effects. Thus the errors reported here and elsewhere may be slightly smaller than the various analyzes suggest.

Can this predicted Landsat data be used for biophysical parameter retrieval or can this approach only be used for land cover, land cover change and visualization applications? For biophysical applications accounting for temporal drift is likely necessary. In this research we attempted to account for this aspect, but do not explicitly evaluate performance. A rigorous approach to evaluating this aspect needs further research and was considered beyond the scope of the objectives here. Comparison with MODIS data suggests that the error was similar to that of the leave one out Landsat assessment and correlation between the predicted Landsat data and MODIS was reasonable for many land cover and feature combinations. Thus, it may be possible to retrieve biophysical parameters with similar thematic accuracy as current MODIS products, but with greater spatial detail. Whether the generic harmonic approach or a more in-depth data assimilation approach should be used will require further research and comparison. A key consideration is that biophysical parameters that depend strongly on the more complex seasonality associated with NIR and SWIR bands (Delbart et al., 2005) will be more difficult to retrieve in the presence of sparse sampling with the methods proposed here. In this effort we elected to model NDVI directly, rather than model the bands and use the results to calculate the index. Our initial experimentation suggested that this was the better approach, as errors in modeling bands can be magnified in calculating the index.

The method requires specification of several parameters. Fine tuning of these may be used to improve model predictions for different regions or to adjust the fit for a specific need. Here we provide a general overview of the importance and sensitivity of these parameters. Not accounting for those associated with residual cloud and shadow screening, parameters are specified for imputation, change detection, and fitting the final harmonic model. Of these, those associated with the final model fit are the most critical. Results are less sensitive to the change detection and imputation parameters. Parameters for change include: the between year change z-score threshold, within year change z-score threshold, and the number of Landsat observations for inclusion of the 2nd order polynomial term. The three-year piecewise approach allows the model to moderately adjust to between year changes, but with larger error than if the change detection methods are applied. Within year changes would not be well represented without the change detection step unless there is a high density of Landsat observations

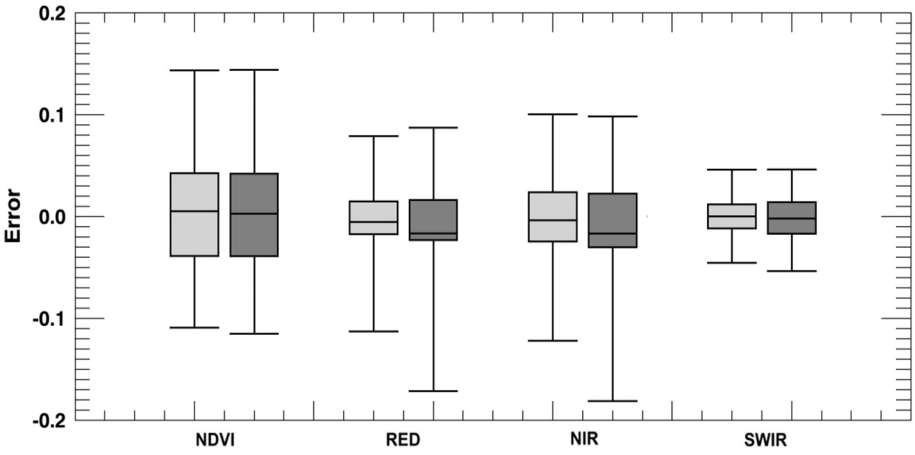


**Fig. 12.** Comparison of model error (climate constrained) associated without change (light grey) and change (dark grey). Box plots are shown as the mean, 25th/75th percentiles, and 5th/95th percentiles.

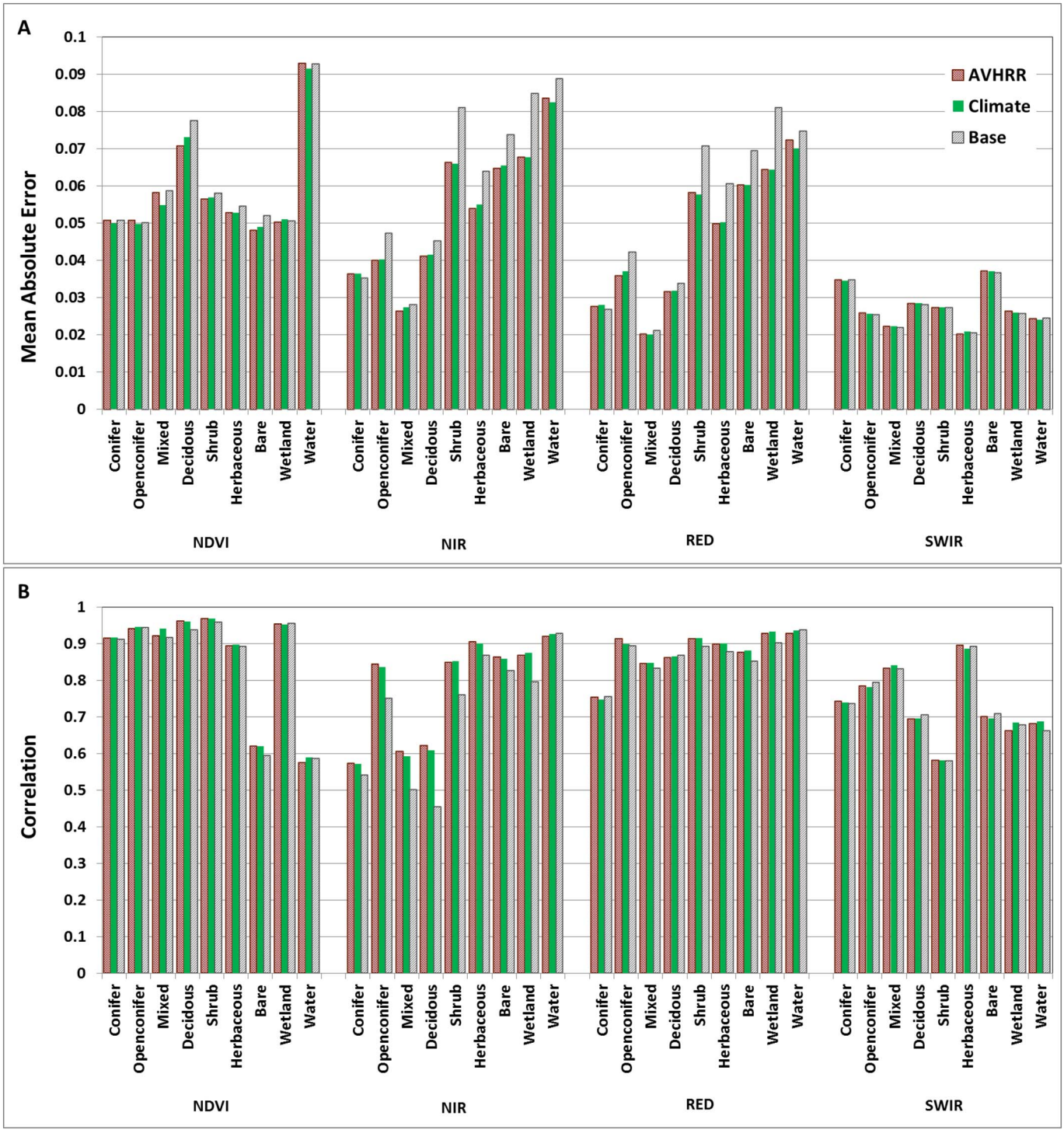


**Fig. 13.** Results of predicted Landsat time series comparison with MODIS for mean absolute error (A) and correlation (B).

(more than 2 within ± 20 days of each date to be predicted). At higher observation densities, additional model terms are included making it more adaptable to within year changes. The polynomial term is only required if capturing anomalous inter-annual variation in yearly maximum or minimum values is of interest. For land cover and land cover changes studies this is generally not required.

Regarding imputation, other formulations of the climate data or a more physically based model could be used to improve imputed predictions. Prediction accuracy along with the imputed temporal density and weight applied to the imputed estimates control the sensitively of the final model predictions to the imputation. In this implementation, imputed values were estimated approximately bimonthly and given a low weight in the final model (0.25). Lower weights (0.15) were assigned to winter months as there were generally few winter Landsat observations available. Thus, the results are only moderately sensitive to the imputed estimates. Using a high weight increases the sensitivity to imputed estimates and thus the importance of the accuracy. To reduce potential overfitting in the imputation, we used a model selection

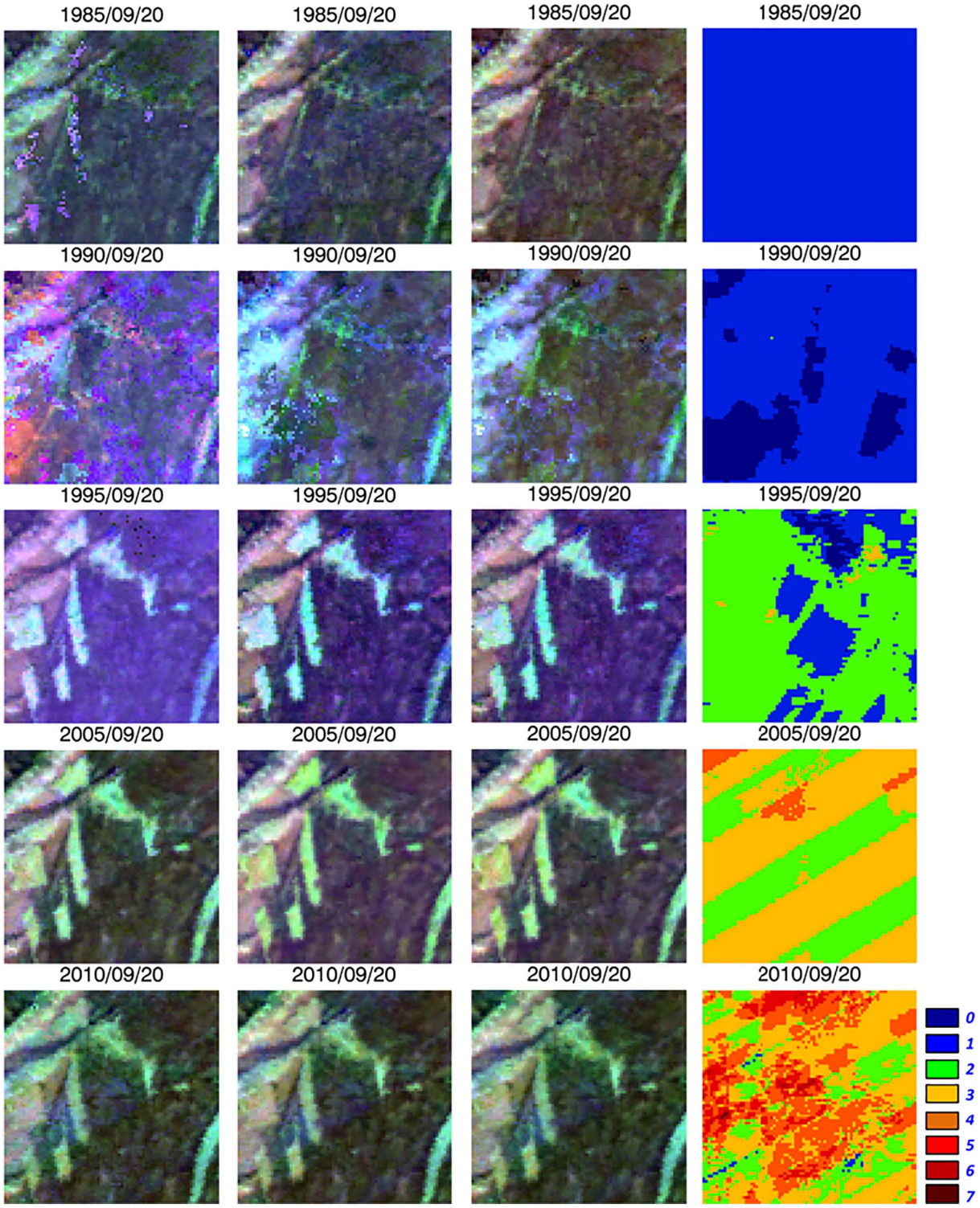


**Fig. 14.** Predicted images for the unconstrained (left), AVHRR constrained (middle), climate constrained (right), and observation density (far right). Color bar represents observation density within ± 20 days. Images are displayed as red = NIR, green = SWIR, and blue = Red.

method based on the percent deviation of model MAE. Other model selection methods could be used based on statistical significance, but this approach was selected for simplicity. Because a low weight was applied to the imputed estimates, this selection method did not have a strong influence on the final model fit.

Parameters for the final model fit included the weights applied to the imputed estimates already discussed, the temporal weight of the Landsat observations by year, and the criteria to add additional harmonic terms to the model based on the number of Landsat observations. In this analysis, we sought the best overall fit for change and no-change segments of the time series and gave the most weight to the central year in the three-year piecewise implementation. However, if change is not of interest then all years can be given a similar weight, which would improve predictions in sparse conditions (less than 3 observations

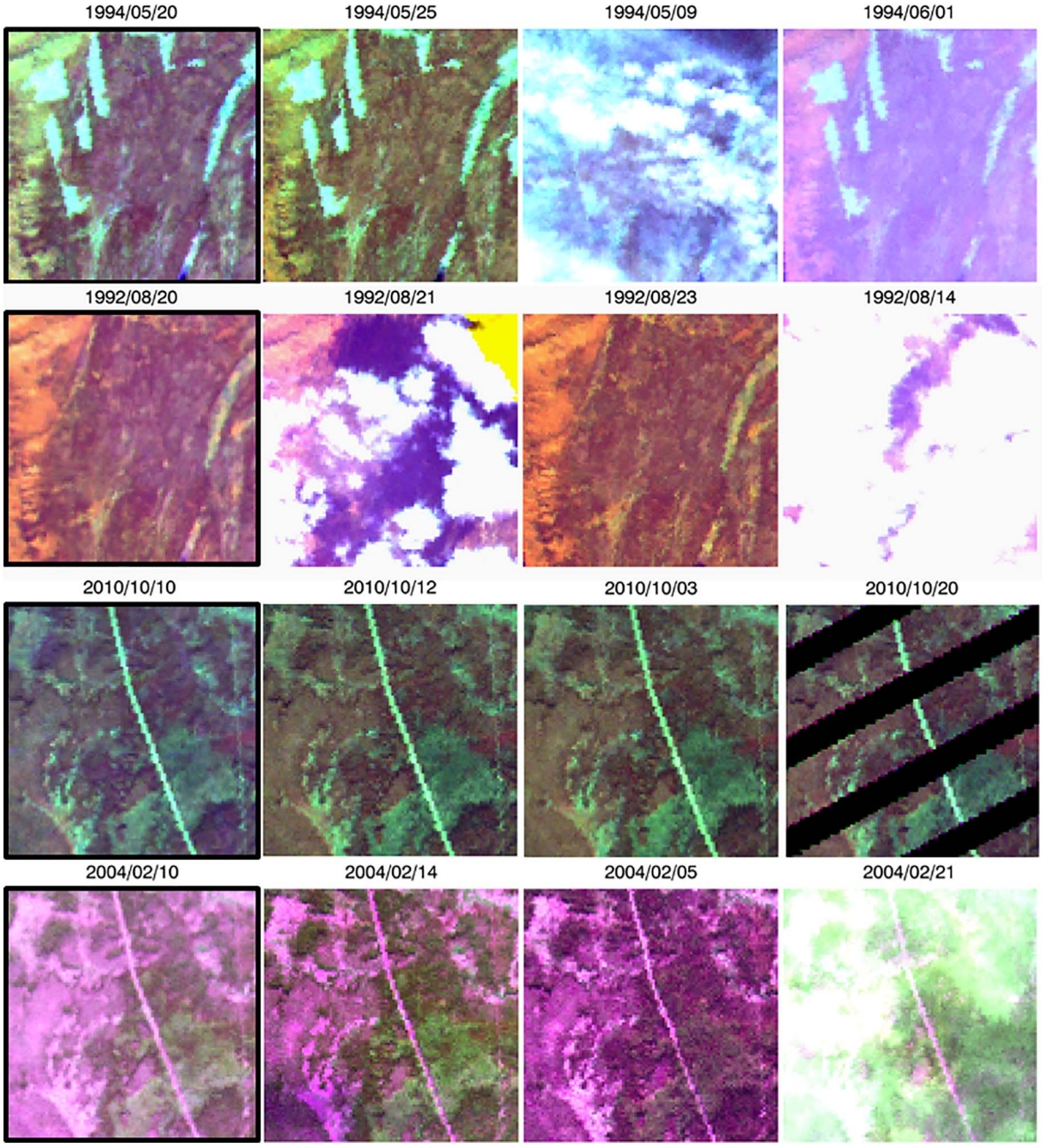


**Fig. 15.** Example comparison with Landsat scenes. The predicted image for each example is outlined on the far left. Images are displayed as red = NIR, green = SWIR, and blue = Red.

within ± 20 days), but this would reduce interannually variability. The criteria to add additional terms were the same as that used in Zhu et al. (2015), except that we adjusted the Landsat observation thresholds to reflect the increased constraint associated with the imputation. This is an important parameter, as it strongly influenced the tendency of the model to over or underfit the data.

Understanding the conditions where time series modeling breaks down is important to develop new methods or identify where new approaches should be investigated. The harmonic modeling method applied to Landsat is relatively new and the interaction between land cover, band, sample sparsity, and error are factors that need to be better understood and accounted for. We have found some limits to understanding the potential for time series reconstruction. Additional improvements on this method include the investigation of different basis functions used for seasonality applications with coarse resolution data (Eklund and Jönsson, 2015), testing different data (e.g. climate grids) and methods of imputation, dynamic parameters and weighting such as adjusting weights for climate data depending on climate suitability or increasing adjacent year weights where change between years is not expected. The method developed here was designed for historical time series reconstruction. However, it is possible to apply it for near-real time applications by using the past two years to aid in modeling the present year's data.

Processing time is an important consideration. The research code developed was not optimized for speed, but developed to examine potential improvement. Further research is planned before embarking on the development of an optimized code implementation. Testing in more northern regions and in complex terrain is considered a priority to better determine the error rate of Landsat time series reconstruction in Canada.

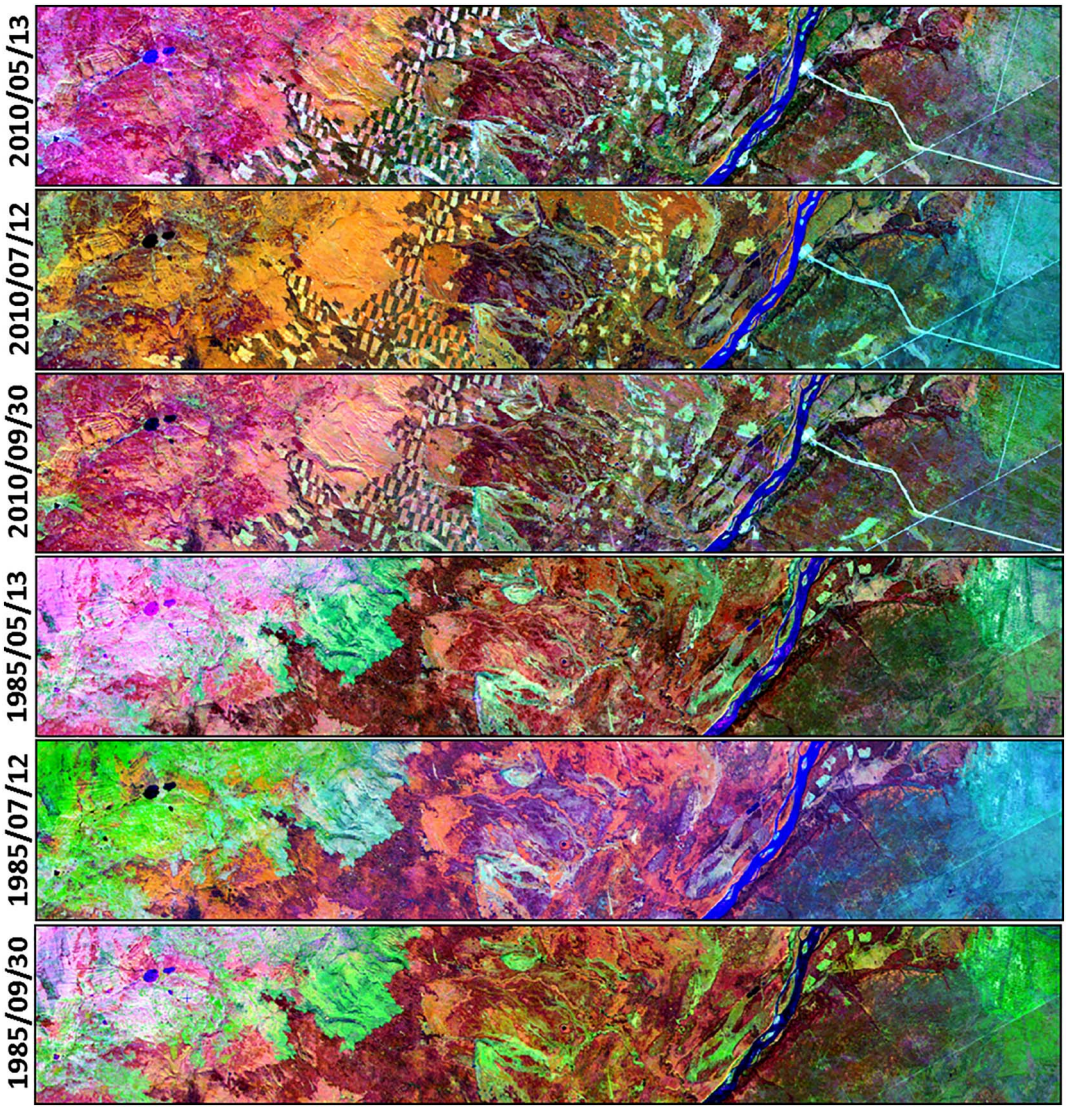


**Fig. 16.** Example seasonal development (spring, summer, fall) and change between 1985 and 2010 for predicted images. Images are displayed as red = NIR, green = SWIR, and blue = Red.

## Acknowledgements

We would like to extend our gratitude to Lixin Sun for his initial review of the manuscript. We would also like to thank the anonymous reviewers for their thoughtful comments.

## References

Borak, J.S., Lambin, E.F., Strahler, A.H., 2000. The use of temporal metrics for land cover change detection at coarse spatial scales. Int. J. Remote Sens. 21, 1415–1432.
Cihlar, J., Ly, H., Li, Z., Chen, J., Pokrant, H., Huang, F., 1997. Multitemporal, multi-channel AVHRR data sets for land biosphere studies—artifacts and corrections. Remote Sens. Environ. 60, 35–57.
Cihlar, J., Latifovic, R., Chen, J., Li, Z., 1999. Testing near-real time detection of contaminated pixels in AVHRR composites. Can. J. Remote. Sens. 25, 160–170.
Cleveland, W.S., 1979. Robust locally weighted regression and smoothing scatterplots. J. Am. Stat. Assoc. 74, 829–836.
Delbart, N., Kergoat, L., Le Toan, T., L'Hermitte, J., Picard, G., 2005. Determination of phenological dates in boreal regions using the normalized difference water index. Remote Sens. Environ. 97, 26–38.
DeVries, B., Verbesselt, J., Kooistra, L., Herold, M., 2015. Robust monitoring of small-scale forest disturbances in a tropical montane forest using Landsat time series. Remote Sens. Environ. 161, 107–121.
Edey, S.N., 1977. Growing Degree Days and Crop Production in Canada. Agriculture Canada Publication 1635/E (ISBN: 0-662-01 138-4).
Eklund, L., Jönsson, P., 2015. TIMESAT: a software package for time-series processing and assessment of vegetation dynamics. In: Kuenzer, C., Dech, S., Wagner, W. (Eds.), Remote Sensing Time Series. Springer International Publishing, pp. 141–158.
Emelyanova, I.V., McVicar, T.R., Van Niel, T.G., Li, L.T., van Dijk, A.I.J.M., 2013. Assessing the accuracy of blending Landsat–MODIS surface reflectances in two landscapes with contrasting spatial and temporal dynamics: a framework for algorithm selection. Remote Sens. Environ. 133, 193–209.
Fisher, J.I., Mustard, J.F., Vadeboncoeur, M.A., 2006. Green leaf phenology at Landsat resolution: scaling from the field to the satellite. Remote Sens. Environ. 100, 265–279.
Fraser, R.H., Abuelgasim, A., Latifovic, R., 2005. A method for detecting large-scale forest cover change using coarse spatial resolution imagery. Remote Sens. Environ. 95, 414–427.
Gao, F., Masek, J., Schwaller, M., Hall, F., 2006. On the blending of the Landsat and MODIS surface reflectance: predicting daily Landsat surface reflectance. IEEE Trans. Geosci. Remote Sens. 44, 2207–2218.
Goward, S., Arvidson, T., Williams, D., Faundeen, J., Irons, J., Franks, S., 2006. Historical record of Landsat global coverage: mission operations, NSLRSDA, and international cooperator stations. Photogramm. Eng. Remote. Sens. 72, 1155–1169.
Hansen, M., Roy, D., Lindquist, E., Adusei, B., Justice, C.O., Altstatt, A., 2008. A method for integrating MODIS and Landsat data for systematic monitoring of forest cover and change in the Congo Basin. Remote Sens. Environ. 112, 2495–2513.
Hilker, T., Wulder, M.A., Coops, N.C., Seitz, N., White, J.C., Gao, F., Masek, J.G., Stenhouse, G.B., 2009. Generation of dense time series synthetic Landsat data through data blending with MODIS using a spatial and temporal adaptive reflectance fusion model. Remote Sens. Environ. 113, 1988–1999.
Holben, B.N., 1986. Characteristics of maximum-value composite images for temporal AVHRR data. Int. J. Remote Sens. 7, 1417–1434.
Hwang, T., Song, C., Bolstad, P.V., Band, L.E., 2011. Downscaling real-time vegetation dynamics by fusing multi-temporal MODIS and Landsat NDVI in topographically complex terrain. Remote Sens. Environ. 115, 2499–2512.
Ju, J., Roy, D.P., 2008. The availability of cloud-free Landsat ETM + data over the

conterminous United States and globally. Remote Sens. Environ. 112, 1196–1211.
Khlopenkov, K.V., Trichtchenko, A.P., 2008. Implementation and evaluation of concurrent gradient search method for reprojection of MODIS level 1B imagery. IEEE Trans. Geosci. Remote Sens. 46, 2016–2027.
King, M.D., Platnick, S., Menzel, W.P., Ackerman, S.A., Hubanks, P.A., 2013. Spatial and temporal distribution of clouds observed by MODIS onboard the Terra and Aqua satellites. IEEE Trans. Geosci. Remote Sens. 51, 3826–3852.
Kovalskyy, V., Roy, D.P., 2013. The global availability of Landsat 5 TM and Landsat 7 ETM + land surface observations and implications for global 30 m Landsat data product generation. Remote Sens. Environ. 130, 280–293.
Lambin, E.F., 1996. Change detection at multiple temporal scales: seasonal and annual variations in landscape variables. Photogramm. Eng. Remote Sens. 62, 931–938.
Latifovic, R., Pouliot, D., 2007. Analysis of climate change impacts on lake ice phenology in Canada using the historical satellite data record. Remote Sens. Environ. 106, 492–507.
Latifovic, R., Pouliot, D., 2013. Correction of bias in AVHRR time series data. In: Global Space-based Inter-Calibration System Quarterly. 7. pp. 4–6.
Latifovic, R., Trichtchenko, A., Chen, J., Park, W., Khlopenkov, K., Fernandes, R., Pouliot, D., Ungureanu, C., Luo, Y., Wang, S., Davidson, A., Cihlar, J., 2005. Generating historical AVHRR 1 km baseline satellite data records over Canada suitable for climate change studies. Can. J. Remote. Sens. 31, 324–348.
Latifovic, R., Pouliot, D., Sun, L., Schwarz, J., Parkinson, W., 2015. Moderate resolution time series data management and analysis: automated large area mosaicking and quality. In: Canada Center for Mapping and Earth Observation, Geomatics Canada Open File, http://dx.doi.org/10.4095/296204.
Lunetta, R.S., Knight, J.F., Ediriwickrema, J., Lyon, J.G., Worthy, L.D., 2006. Land-cover change detection using multi-temporal MODIS NDVI data. Remote Sens. Environ. 105, 142–154.
Luo, Y., Trichtchenko, A.P., Khlopenkov, K.V., 2008. Developing clear-sky, cloud and cloud shadow mask for producing clear-sky composites at 250-meter spatial resolution for the seven MODIS land bands over Canada and North America. Remote Sens. Environ. 112, 4167–4185.
Lyapustin, A., Wang, Y., Frey, R., 2008. An automatic cloud mask algorithm based on time series of MODIS measurements. J. Geophys. Res.-Atmos. 113 (2008), D16207.
Melaas, E.K., Friedl, M.A., Zhu, Z., 2013. Detecting interannual variation in deciduous broadleaf forest phenology using Landsat TM/ETM + data. Remote Sens. Environ. 132, 176–185.
Pouliot, D., Latifovic, R., 2016. Land change attribution based on Landsat time series and ancillary disturbance data integration in the Athabasca oil sands region. GISci. Remote. Sens. 53, 382–401.
Pouliot, D., Latifovic, R., Fernandes, R., Olthof, I., 2009a. Evaluation of annual forest disturbance monitoring using decision trees and MODIS 250 m data. Remote Sens. Environ. 113, 1749–1759.
Pouliot, D., Latifovic, R., Olthof, I., 2009b. Trends in vegetation NDVI from 1 km AVHRR data over Canada for the period 1985–2006. Int. J. Remote Sens. 30, 149–168.
Pouliot, D., Latifovic, R., Fernandes, R., Olthof, I., 2010. Evaluation of compositing period and AVHRR and MERIS combination for improvement of spring phenology detection in deciduous forests. Remote Sens. Environ. 115, 158–166.
Pouliot, D., Latifovic, R., Zabcic, N., Guindon, L., Olthof, I., 2013. Development and assessment of a 250 m spatial resolution MODIS annual land cover time series (2000 − 2011) for the forest region of Canada derived from change-based updating. Remote Sens. Environ. 140, 731–743.
Press, W.H., Flannery, B.P., Teukolsky, S.A., Vetterling, W.T., 1992. Numerical Recipes in FORTRAN: The Art of Scientific Computing, 2nd ed. Cambridge University Press, Cambridge, England, pp. 697.
Ramsay, B., 1998. The interactive multisensor snow and ice mapping system. Hydrol. Process. 12, 1537–1546.
Rossow, W.B., Garder, L.C., 1993. Cloud detection using satellite measurements of infrared and visible radiances for ISCCP. J. Clim. 6, 2341–2369.
Small, C., 2004. The Landsat ETM + spectral mixing space. Remote Sens. Environ. 93, 1–17.
Trichtchenko, A.P., Luo, Y., Khlopenkov, K.V., 2006. A method for downscaling MODIS land channels to 250 m spatial resolution using adaptive regression and normalization. Proc. SPIE Int. Soc. Opt. Eng. 6366 (2006) (art. no. 636607 8 pp).
Verbesselt, J., Hyndman, R., Newnham, G., Culvenor, D., 2010. Detecting trend and seasonal changes in satellite image time series. Remote Sens. Environ. 114, 106–115.
Verbesselt, J., Zeileis, A., Herold, M., 2012. Near Real-time Disturbance Detection Using.
White, M.A., Thornton, P.E., Running, S.W., 1997. A continental phenology model for monitoring vegetation responses to interannual climatic variability. Glob. Biogeochem. Cycles 11, 217–234.
White, M.A., de Beurs, K.M., Didan, K., Inouye, D.W., Richardson, A.D., Jensen, O.P., O'Keefe, J., Zhang, G., Nemani, R.R., van Leeuwen, W.J.D., Brown, J.F., de Wit, A., Schaepman, M., Lin, X., Dettinger, M., Bailey, A.S., Kimball, J., Schwartz, M.D., Baldocchi, D.D., Lee, J.T., Lauenroth, W.K., 2009. Intercomparison, interpretation, and assessment of spring phenology in North America estimated from remote sensing for 1982 to 2006. Glob. Chang. Biol. 15, 2335–2359.
Zhan, X., DeFries, R., Townshend, J.R.G., DiMiceli, C., Hansen, M., Huang, C., Sohlberg, R., 2000. The 250 m global land cover change product from the moderate resolution imaging spectroradiometer of NASA's earth observing system. Int. J. Remote Sens. 21, 1433–1460.
Zhang, X., Friedl, M.A., Schaaf, C.B., Strahler, A.H., Hodges, J.C.F., Gao, F., Reed, B.C., Huete, A., 2003. Monitoring vegetation phenology using MODIS. Remote Sens. Environ. 84, 471–475.
Zhao, H., Fernandes, R., 2009. Daily snow cover estimation from advanced very high resolution radiometer polar pathfinder data over northern hemisphere land surfaces during 1982–2004. J. Geophys. Res. 114, D05113.
Zhu, Z., Woodcock, C.E., 2014a. Automated cloud, cloud shadow, and snow detection in multitemporal Landsat data: an algorithm designed specifically for monitoring land cover change. Remote Sens. Environ. 152, 217–234.
Zhu, Z., Woodcock, C.E., 2014b. Continuous change detection and classification of land cover using all available Landsat data. Remote Sens. Environ. 144, 152–171.
Zhu, X., Chen, J., Gao, F., Chen, X., Masek, J.G., 2010. An enhanced spatial and temporal adaptive reflectance fusion model for complex heterogeneous regions. Remote Sens. Environ. 114, 2610–2623.
Zhu, Z., Woodcock, C.E., Olofsson, P., 2012. Continuous monitoring of forest disturbance using all available Landsat imagery. Remote Sens. Environ. 122, 75–91.
Zhu, Z., Woodcock, C.E., Holden, C., Yang, Z., 2015. Generating synthetic Landsat images based on all available Landsat data: predicting Landsat surface reflectance at any given time. Remote Sens. Environ. 162, 67–83.